Proceedings of the
International Conference on

Duality and Symmetry in Hadron Physics

Edited by

E. GOTSMAN

Department of Physics and Astromony

Tel Aviv University

THE WEIZMANN SCIENCE PRESS OF ISRAEL

2

Many Particle Phenomena*

D. HORN**

1. INTRODUCTION

THE PURPOSE of this paper is to discuss several interesting problems in the field of many particle production that have received a good deal of attention lately. Since this is not intended to be a review paper, several theories as well as important experimental observations are not mentioned. For recent experimental and theoretical summaries that also cover the topics that we omit we refer the reader to: A. Wroblewski, Rapporteur's Talk at the Kiev Conference; L. Van Hove, Phys. Rep. **1**, 347 (1971); and H. Grote, R. Hagedon and J. Ranft, Particle Spectra, CERN, 1970.

At the price of limiting the scope of the paper we have tried to discuss at length several controversial topics. We have emphasized a simple statement of the principles and consequences of the theories and their comparison with experimental results. Since this subject started gaining popularity only recently we start from first principles—review of the important experimental facts—and work our way up.

2. GENERAL PROPERTIES

A. Abundance of Pions

A striking fact is that most particles that are produced in the high energy collisions are pions. Thus, e.g., at 25 BeV $\pi^- p$ re-

* Work supported in part by the U.S. National Bureau of Standards.

** Department of Physics and Astronomy, Tel Aviv University, Tel Aviv.

actions,[1] only 16% of the produced channels include strange particle production. Even these strange particles are usually accompanied by pions. Thus the problem at hand is far from being close to the $SU(3)$ limit. This is so although the sums of the various cross sections, namely the total cross sections, do obey many symmetry relations. When we discuss many particle production we are treating mainly the production of many pions together with one or two baryons as determined by the incoming particles.

B. Poisson Type Distributions

A typical distribution[2] of the cross sections for the production of non-strange particles in 16 BeV $\pi^- p$ reactions is plotted in Fig. 1 vs the number of prongs observed. They fall on a curve similar to a Poisson distribution. There are many papers on the

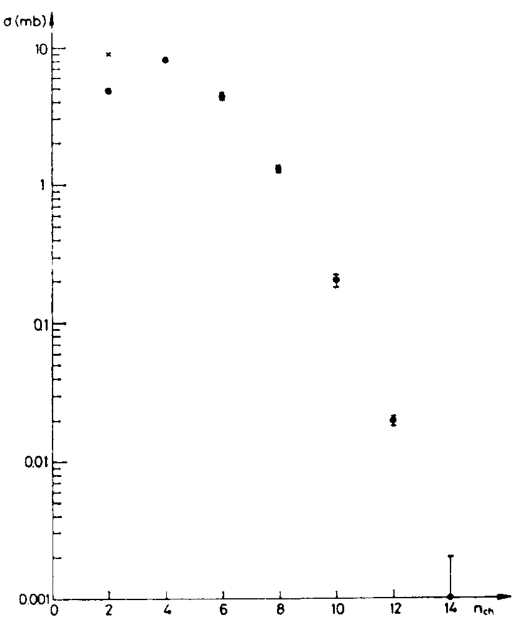

Fig. 1. Cross sections for non-strange particle production in 16 BeV $\pi^- p$ collisions (from Ref. 2) plotted vs the number of prongs. The curve has the characteristic shape of a Poisson distribution. The cross (×) at $n_{ch} = 2$ corresponds o the value of σ that includes the elastic cross section while the circle designates only the inelastic cross section.

question of whether it is really a Poisson distribution, and if so in which variable. In order to avoid this problem we call it a "Poisson-type" distribution referring to the characteristic structure of a broad peak for low values of $\langle n_c \rangle$ and a steep fall for higher values. One normally leaves out the elastic cross section from these plots regarding it later as the shadow of all inelastic channels. The elastic point is added in the figure for comparison.

C. Low Transverse Momenta

The transverse momenta (p_T) of the outgoing particles are usually of the order of 300 MeV or so and do not change appreciably with the change in incoming energy. The process can therefore be described within a cylinder in momentum space. This is shown in Figs. 2 and 3 which also emphasize the two characteristic modes of production:

D. Leading Particles and Pionization

Note that in Fig. 2 the proton distribution is clearly concentrated near the location of the incoming (target) proton. The π^- distribution (there are two π^- produced) has a strong tail in the direction

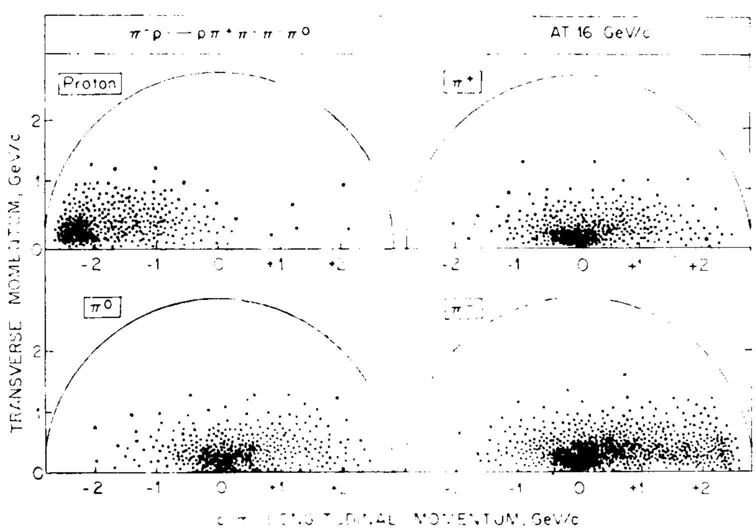

Fig. 2. Peyrou plot of 16 BeV $\pi^-p \to \pi^-p\pi^-\pi^0\pi^+$ taken from Ref. 2.

of the incoming π^-. These two particles that follow the trend of the incoming particles are referred to as "leading particles". In contrast one finds all other pions around the CM origin. This phenomenon, namely the existence of a cloud of pions with low CM longitudinal momenta (p_L) is sometimes referred to as pionization. The same name is reserved by some authors for a different use—describing a concentration of pions around the CM that stays finite as one increases the incoming energy indefinitely. One has therefore to be cautious when one uses this term in heated discussion.

The description of the process in momentum space has one deceiving aspect to it, namely, one may tend to think that this separation between the leading proton and all the pions exists in configuration space. This is not true since if a proton and a

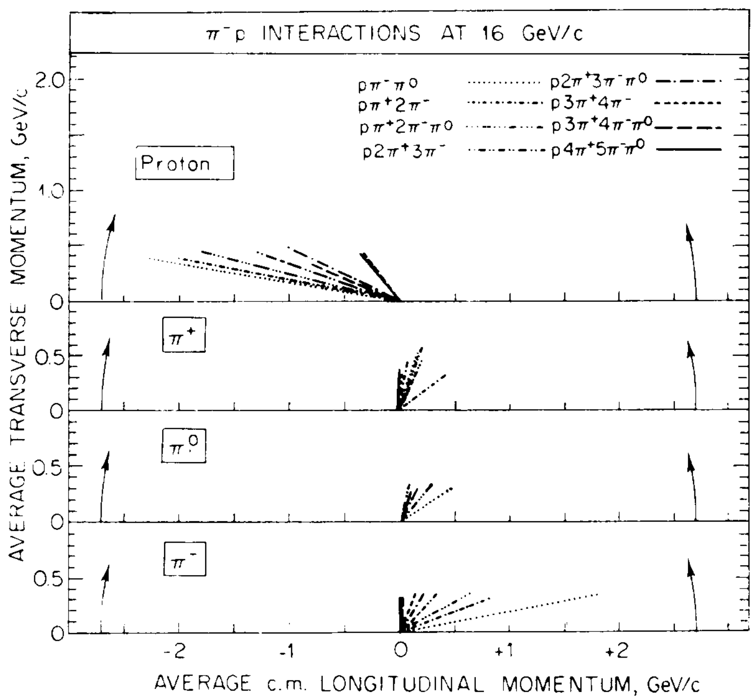

Fig. 3. Vectors of average momenta of various particles in different modes observed in 16 BeV π^-p collisions (from Ref. 2).

pion move with the same velocity the ratio between their two momenta is m_p/m_π thus strongly favouring a separation in momentum space. That says also that Fig. 2 does not preclude the existence of resonances in intermediate stages which then decay into the proton and pions.

Figure 3 shows the average momentum of the outcoming particles as a function of the multiplicity. One sees again the clear cutoff in p_T. We note also the decrease in the leading particle effect as the multiplicity increases.

An exception to the rule of leading particles is given by $\bar{p}p$ annihilation and we may justly ask ourselves whether the $\bar{p}p$ reactions fall into the same class with the πp and pp ones where annihilation is absent. Figure 4 shows the relative importance of the various types of channels in $\bar{p}p$ reactions. The total annihilation cross section is falling with energy (as indicated on the figure) presumably like some power of the incoming energy. We may

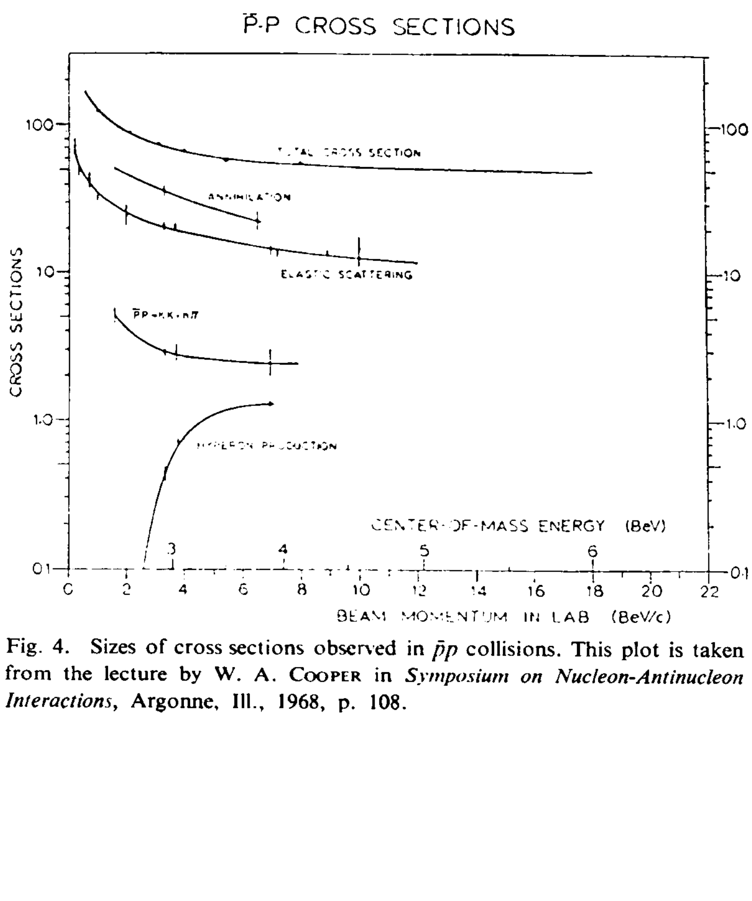

Fig. 4. Sizes of cross sections observed in $\bar{p}p$ collisions. This plot is taken from the lecture by W. A. Cooper in *Symposium on Nucleon-Antinucleon Interactions*, Argonne, Ill., 1968, p. 108.

expect that at higher energies the $\bar{p}p$ reactions will resemble more and more the pp ones. The proportion of the elastic vs the total cross sections as well as strange particle production is similar to that observed for other incoming particles when absorption channels are absent.

E. Increase of the Average Multiplicity

The last point that we want to emphasize in this section is the logarithmic increase of the average produced multiplicity with the incoming energy. Recent cosmic-rays data[3] at energies that will be soon available also in NAL and ISR are shown in Fig. 5 and verify that the increase of $\langle n_c \rangle$ is logarithmic in this energy range.

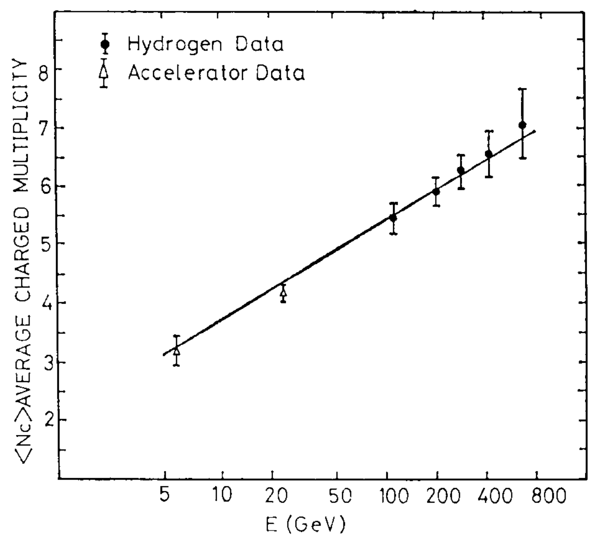

Fig. 5. The average charged multiplicity in the pp cosmic rays experiment[3] which shows a logarithmic increase with energy.

3. THE MULTIPERIPHERAL MODEL

The logarithmic increase of the multiplicity is one of the well-known results of the multiperipheral model. This model, otherwise known as the ABFST model,[4] was suggested in 1962 and is a straightforward generalization of the peripheral approach to two particle production amplitudes. A scattering amplitude is described by a diagram of the form of Fig. 6. The two question marks refer to the two basic questions—what is exchanged and what is produced. We know that eventually one observes pions, nevertheless it may be that they come mainly in forms of ρ and perhaps σ mesons. We will return to this question of correlations between the pions in the last section. Let us just note here that a model of such meson production would be consistent with pion exchanges. Indeed the original ABFST model dealt with pion exchanges. It was of course soon generalized to include Regge pole exchanges.[5] The trouble with the multi-Regge-exchange model is that its application can be justified only for about 10% of the data at conventional energies.[6] Although several successful modifications have been suggested, such as the CLA model[7] and multi-Veneziano formulae,[8] we have seen a return to the old pion-exchange models in the last two years.[9]

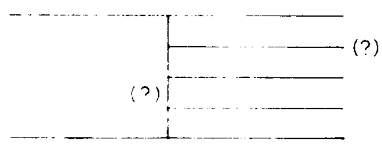

Fig. 6. Multiperipheral diagram.

The arguments that we are going to bring here and the derivation of the logarithmic increase of the multiplicity, are quite general and independent of the exact details of the model. We follow Fubini[10] and note that if one changes all the coupling constants by a continuous parameter then all n-particle cross sections (σ_n) will change accordingly as

$$\sigma_n \rightarrow \lambda^n \sigma_n \qquad \sigma_T = \sum_{n=2}^{\infty} \sigma_n \rightarrow \sum_{n=2}^{\infty} \lambda^n \sigma_n \tag{1}$$

It follows from Eq. (1) that

$$\langle n \rangle = \frac{\lambda}{\sigma_T} \frac{\partial}{\partial \lambda} \sigma_T \bigg|_{\lambda=1} \tag{2}$$

We assume now that the total cross section has a leading power behaviour, namely

$$\sigma_T(\lambda) \simeq \beta(\lambda) s^{\alpha(\lambda)-1}$$

and the choice $\lambda = 1$ leads to the expected asymptotic result $\alpha = 1$. It follows then that

$$\langle n \rangle = \left(\lambda \alpha'(\lambda) \ln s + \frac{\lambda \beta'(\lambda)}{\beta(\lambda)} \right) \Big|_{\lambda=1} = a \ln s + b \tag{4}$$

Two main assumptions went into this calculation: The first is that there exists a simple basic mechanism by which all cross sections change proportionally. This is characteristic of independent production as well as quasi-independent mechanisms like the multiperipheral model. This leads also to Poisson-like distributions of the type discussed in the previous section. The second assumption is that of the leading power behaviour. Within a specific multiperipheral model one can of course calculate explicitly the various cross sections. Figure 7 shows the results of such a calculation by Wyld[11] who looked at $\pi\pi \to n\rho$ mesons via pion exchanges. He calculated the resulting Feynman diagrams using the physical masses of the ρ and π and varying the $\rho\pi\pi$ coupling constant until a constant asymptotic σ_T was reached. We note how quickly σ_T reaches its constant value. The calculation fixes the $\rho\pi\pi$ coupling constant and the total cross section. Both come out much too big. The discrepancy in the orders of magnitude prevails also in more sophisticated versions of this model.[12] Recently Abarbanel et al.[13] suggested an interpretation that circumvents this difficulty. They looked at pseudo-scalar scattering that results in vector-meson production, both being part of unitary symmetry multiplets. They looked for the leading singularity in a Bethe Salpeter equation—the equivalent of summing all diagrams of the type of Fig. 6. The only parameter left in their problem was M_v—the mass of the vector mesons, and they derive the result

$$\sigma_T = \frac{16\pi^3}{N} \frac{1}{M_v^2} \tag{5}$$

where N is the dimensionality of the multiplet. By choosing

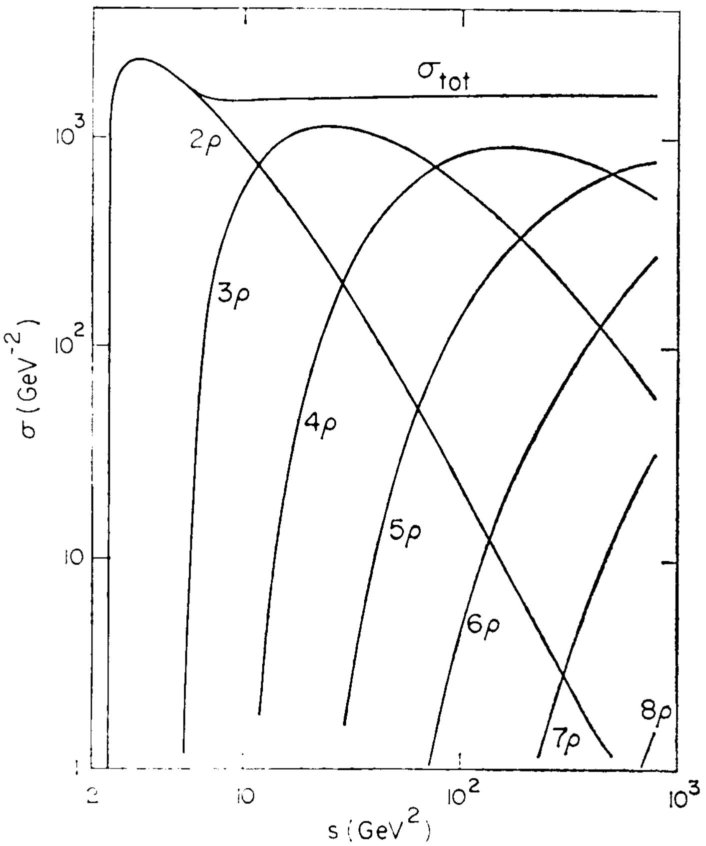

Fig. 7. Results of a multiperipheral calculation by Wyld[11] of the process $\pi\pi \to n\rho = np$ $n = 2, 3, \ldots$ based on elementary pion exchange. The only free parameter was the $\rho\pi\pi$ coupling which was chosen so as to give an asymptotic constant total cross section.

$N = 8$ and $M_v = 900$ MeV one gets $\sigma_T = 30$ mb. Although the resulting σ_T has a reasonable magnitude one has to remember that the actual situation is very far from the $SU(3)$ limit—as already stressed in the previous section. One may therefore doubt whether this can be regarded as a realistic derivation of the observed magnitude of the total cross section.

The big advantage of the multiperipheral model, in any of its many variations, is that it is the only simple generalization of the known techniques for two particle production. Although detailed predictions may fail in experimental applications of the model, it still may serve as a guide to our intuition when discussing the complex phenomena of many particle production.

4. SIMPLE DYNAMICS AND KINEMATICS

One of the predictions of the multiperipheral model is that the cross section for any specific channel will behave as

$$\sigma = \nu^{2\alpha-2} \tag{6}$$

where ν is the incident energy in the laboratory. This is an asymptotic result where α is some average Regge intercept of the various exchanges. A recent analysis of 64 reactions by Hansen, Kittel and Morrison[14] shows that the energy behaviour of the various cross sections is indeed specified by the exchanged quantum numbers rather than, say, the multiplicity of particles observed. Their analysis is summarized in Table 1.

Table 1
Energy Behaviour of Cross Sections

Reaction	Exchange	α
$(\pi, K, p) + p \to (\pi, K, N) + N$ + pions	Meson $S=0$	0
$K^-p \to \Lambda$ + pions	Meson $S=1$	$-\frac{1}{2}$
$K^-p \to \Xi + K$ + pions	Baryon $S=0$	-1

To derive their results the authors used a trick, namely, they looked at σ_A defined by

$$\sigma_A \propto \sigma \frac{\nu^{n-2}}{\text{Phase Space}} \tag{7}$$

rather than at the cross section σ. n is the multiplicity of the channel discussed and A stands for "asymptotic" since asymptotically the phase space term behaves like ν^{n-2}. The behaviour of σ and σ_A for a particular channel is shown in Fig. 8. We see that the effect of the multiplicative factor in (7) is to raise the lower part of σ and, miraculously enough, it leads to simple power behaviour from low energies onward.

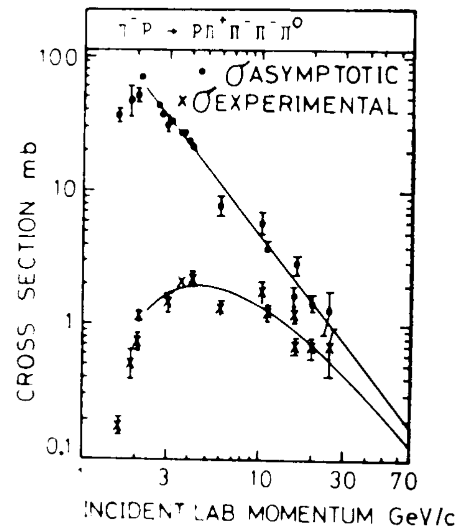

Fig. 8. Characteristic variation of a cross section (σ) with energy and the quantity σ_A defined in Eq. (7). Taken from Ref. 14.

The phase space term referred to above is given by the Lorentz invariant expression

$$\text{P.S.} = \int \prod_i \frac{d^3 p_i}{E_i} \delta^{(3)}\left(\sum_i \vec{p}_i\right) \delta\left(\sum_i E_i - W\right) = W^{2n-4} F_{ps}\left(\frac{W}{\mu}\right) \quad (8)$$

where we used the momenta and energies in CM and $W = \sqrt{s}$ is the total CM energy. If one assumes for simplicity that all particles have the same mass μ then one can prove the rhs equality. The function $F_{ps}(W/\mu)$ is regular in the limit $\mu \to 0$ or $W \to \infty$ and therefore the asymptotic behaviour of PS is like W^{2n-4} or ν^{n-2}. Obviously σ does not behave like PS since it is decreasing with energy. We know already from the general properties listed in Section 2 that phase-space is far from being homogeneously filled. Figures 2 and 3 demonstrate clearly the strong cutoff in the transverse momentum. If one introduces such a cutoff into the PS formula it will lead to

$$\text{P.S.} \xrightarrow{p_T<K} W^{2n-4}\left(\frac{K}{W}\right)^{2n-2} F\left(\frac{W}{\mu}, \frac{W}{K}, \frac{K}{\mu}\right) \tag{9}$$

which has a leading W^{-2} behaviour provided F is a regular function in W. To facilitate calculations one might try instead of this more realistic PS formula an approximate expression in which all particles have a fixed (and common) transverse momentum

$$f_n = \int \prod_{i=1}^{n} \frac{dp_{L_i}}{E_i} \delta\left(\sum_i p_i\right) \delta\left(\sum_i E_i - W\right) = \frac{1}{W^2} F_n\left(\frac{W}{m_T}\right) \tag{10}$$

where $m_T^2 = \mu^2 + p_T^2$. Once again we see the decreasing W^{-2} behaviour. The function $F_n(x)$ behaves roughly like $(\ln x)^{n-2}$ and leads therefore to a structure[15] shown in Fig. 9. We note

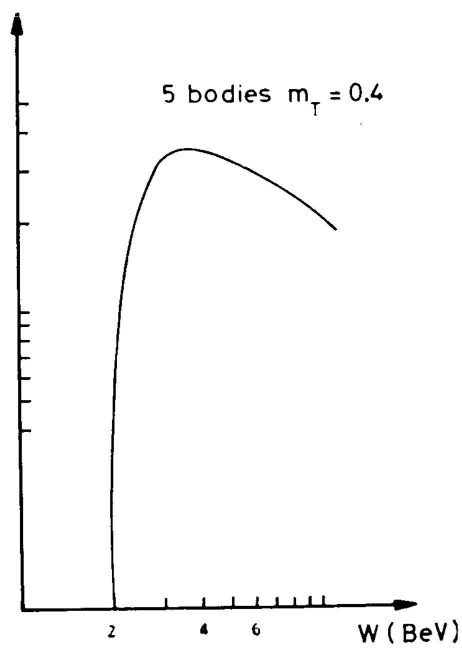

Fig. 9. The variation of longitudinal phase space, Eq. (10), with total CM energy W.

that the shape is very similar to that of σ in Fig. 8. One may therefore correlate the fall of the cross section with the dynamical bounds on the available transverse momenta.

The emerging picture of the high energy processes confines the physical phenomena to a cylinder in momentum space. One may look at the processes from different frames of reference that are related by longitudinal boosts along the axis of this cylinder. In order to develop an understanding that is not tied down to a particular frame of reference we have to define suitable invariant variables. Such a variable is the rapidity[16] z whose relation to the conventional variables is given by

$$\begin{aligned} m_T &= \sqrt{m^2 + p_T^2} \qquad && \beta_L = \frac{p_L}{E} = \tanh z \\ p_L &= m_T \sinh z && \frac{E \pm p_L}{m_T} = e^{\pm z} \qquad (11) \\ E &= m_L \cosh z && \end{aligned}$$

where m_T is referred to as the "transverse mass" and all variables are defined in CM. A longitudinal boost is equivalent to the linear transformation $z \to z - z_0$ and the Lorentz invariant differential element of phase space is $dp_L/E = dz$. The relation between the various quantities defined in (11) is demonstrated in Fig. 10. The points A, B, C denote characteristic values of longitudinal momenta of pions (A, B) and a proton (C) that have the same rapidity (and same velocity). We note the separation between them that was mentioned in Section 2. Whereas the velocity (β_L) can vary only between -1 and 1, the rapidity has an indefinite range (practically between $\pm \ln W/m_T$). A recent review by Wilson[16] describes a picture due to Feynman that views the many particle system as a gas with short-range forces between its constituents (pions) confined in the cylinder of phase space available for the process. Such a picture would predict a homogeneous distribution in z. The same conclusion comes from an interpretation of the two colliding particles as composite objects which, therefore, have no preferred centre.[17] Also the multiperipheral model envisages[10] a homogeneous distribution in z; The most favoured configuration resulting from a diagram like Fig. 6 in

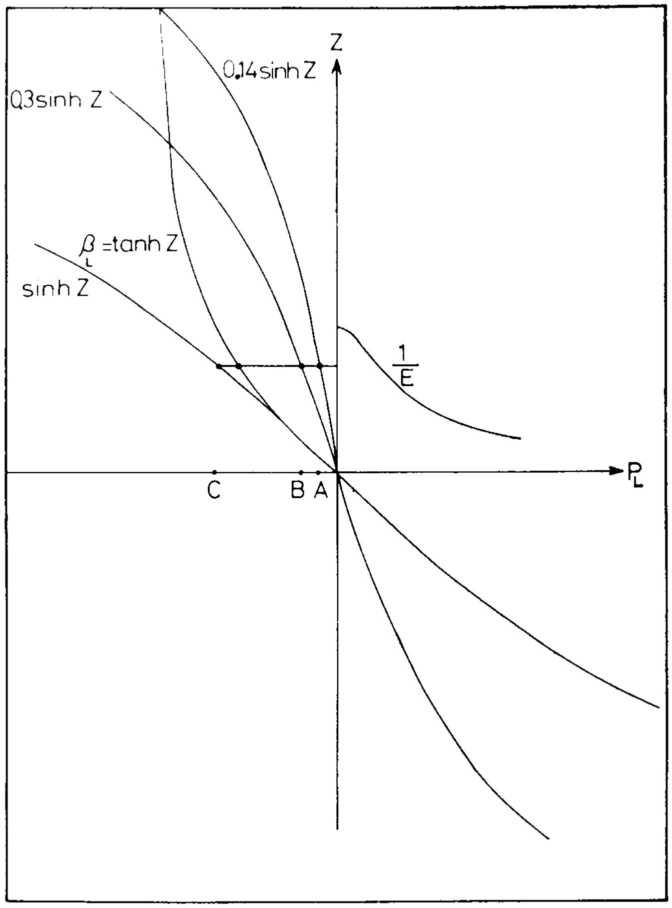

Fig. 10. Diagramatic relation of the rapidity z to momentum variables. The points A and B denote characteristic momentum values of pions which have the same longitudinal velocity as a proton of $p_L = C$. The $1/E$ curve is the momentum distribut:on of phase space (homogeneous z distribution).

asymptotic energies is when all $p_T = 0$ and the consecutively emitted particles have corresponding decreasing values of rapidity with a constant difference between neighbouring particles. An even distribution in z corresponds to a momentum distribution that looks like $1/E$ since $dz = dp_L/E$. Such a curve is plotted in Fig. 10. Viewed in the CM frame one will therefore see a peak around $p_L = 0$ however the same peaking will also be seen in any other (close) frame of reference. This shows the importance of plotting the distribution in rapidity in order to get an invariant understanding of where the distribution peaks, if it peaks at all. Are the expectations of the above-mentioned models born out by present accelerator data? The answer is no, the centre of mass point is still privileged after all. The details of the distributions in momentum space are discussed in the next sections.

5. DISTRIBUTIONS IN MOMENTUM SPACE

Let us start this section by looking at experimental data.[18] Figure 11 shows the cross section for π^- production in 28.5 BeV pp collisions. We see the cross sections for various numbers of prongs and for various cuts in p_T plotted vs p_L in (CM) together with fits by simple exponential functions. We note three important features:

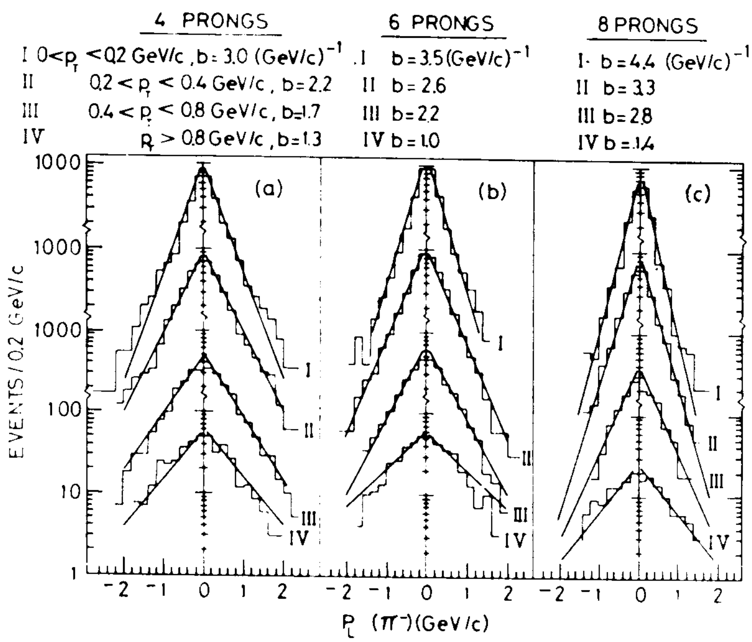

Fig. 11. π^- momentum distribution in 28.5 BeV pp collisions, from Ref. 18.

1) The strong peaking around $p_L = 0$ precludes a simple phase space E^{-1} behaviour.

2) The slope of the functions increases as the number of prongs increases.

3) The slope decreases as p_T increases. This fact means also that the average p_T is smallest at $p_L = 0$ and increases slightly as p_L increases.

The first point is the most relevant one to the question raised at the end of the previous section. One may of course wonder whether this strong peaking is not due to a collective phase-space effect of all other particles in the process that distorts the original E^{-1} behaviour of the single particle distribution. To be able to answer this question we have first to formulate it mathematically. Let us start by defining a Lorentz-invariant distribution in momentum space

$$\rho_i(\vec{p}) = E_i \frac{d^3\sigma}{d^3p_i} \tag{12}$$

where i designates a particle of type i (e.g. π^-) and σ is a cross section out of which ρ is extracted. If σ happens to be the total cross section (σ_T) one discusses the inclusive distribution ρ^T. We may of course restrict ourselves to certain partial cross sections (e.g. $pp \to \pi^- + 3$ prongs) or even a single channel σ_c (e.g. $pp \to pp\pi^-\pi^+\pi^0$). The use of the Lorentz-invariant quantity (12) enables us to eliminate the effect of the phase-space factor. Let us concentrate for a moment on σ_c.

It can be described by

$$\sigma_c = \int g_c(p_1 \cdots p_n, \vec{q}, W) \frac{d^3p_1}{E_1} \cdots \frac{d^3p_n}{E_n} \delta^{(3)}\left(\sum_{i=1}^{n} \vec{p}_i\right) \delta\left(\sum_{i=1}^{n} E_i - W\right) \tag{13}$$

where $p_1 \cdots p_n$ are the momenta of the emitted particles, W the total CM energy and $\vec{q}$ the CM momentum of the target. The function g_c corresponds to the square of the wave-function in momentum space. An (exclusive) experiment that will give us all possible information on this function is out of the question since the number of (momentum) variables grows so quickly that it makes such a prospect unfeasible. We therefore look first at a distribution of the kind

$$\rho_i^c(\vec{p}) = E_i \frac{d^3\sigma_c}{dp_{L_i} d^2 p_{T_i}} =$$

$$n_i \int g_c(p_1 \cdots p_n, \vec{q}, W) \frac{d^3 p_2}{E_2} \cdots \frac{d^3 p_n}{E_n} \delta^{(3)}\left(\sum_{j=1}^{n} \vec{p}_j\right) \delta\left(\sum_{j=1}^{n} E_j - W\right) \tag{14}$$

where we assumed that particle 1 was of type i. n_i is the number of particles of type i in g_c. The distribution $\rho_{ic}(p)$ reflects both the structure of g_c as well as the restrictions imposed by momentum conservation. The latter ones will also affect $\rho_i(\vec{p})$ (defined for any partial cross section) as well as the inclusive $\rho_i^T(\vec{p})$. Our intuitive feeling is that the higher the energy in question the less important the phase-space restrictions become. Let us prove that this is the case.

We limit ourselves first to the line $p_T = 0$. Let us now define

$$\sigma_A(W) = \tag{15}$$

$$\sum_{n,\alpha} \int g(p_1 \cdots p_n, \alpha, \vec{q}, W) \delta^{(3)}\left(\sum_{j=1}^{n} \vec{p}_j\right) \delta\left(\sum_{j=1}^{n} E_j - W\right) \frac{d^3 p_1}{E_1} \cdots \frac{d^3 p_n}{E_n}$$

where α is the set of quantum numbers required by a condition A (like "4 prongs"). We then look at

$$\rho_i(p_L, 0) =$$

$$\langle n_i \rangle E_1 \frac{d^3\sigma_A}{d^3 p_1}\bigg|_{p_{T_1}=0} = \sum_{n,\alpha} n_i \int g(p_1 \cdots p_n, \alpha, \vec{q}, W) \delta^{(3)}\left(\sum_{j=1}^{n} \vec{p}_j\right) \tag{16}$$

$$\times \delta\left(\sum_{j=1}^{n} E_j - W\right) \frac{d^3 p_2}{E_2} \cdots \frac{d^3 p_n}{E_n}\bigg|_{p_{T_1}=0}$$

Since we look for the effect of energy momentum conservation let us assume for a moment that the various g are constant. In other words we test the assumption that the dependence on p_1 is just given by longitudinal phase space. In this case Eq. (16) leads to

$$\rho_i(p_L, p_T = 0) = f(\sqrt{W^2 - 2WE_1 + m_1{}^2}) = f(\mathcal{M}) \tag{17}$$

where $\mathscr{M}$ is the missing-mass of all other particles emitted in addition to particle 1:

$$\mathscr{M} = \sqrt{W^2 - 2WE_1 + m_1^2} \approx W\left(1 - \frac{E_1}{W}\right) \qquad (18)$$

Equation (18) shows that for high values of W, such that $E_1 \ll W$, $\rho_i(p_L, p_T = 0)$ will be roughly a constant reflecting the assumption of a constant g. This corresponds to the intuitive understanding that for high values of available energies the effects of the other particles do not interfere with the distribution of the particle in question. In the data shown in Fig. 11 we discuss values of W that are of order of 7 BeV and E of order of 1 or 2 BeV. If we want a big modification we need a steep function $f(\mathscr{M})$. Before turning to the quantitative analysis let us just note the general characteristic that a peak at $p_L = 0$ means a tendency to produce the highest possible $\mathscr{M}$.

Our specific problem, π^- distributions in pp reactions, has an obvious right-left symmetry in p_L. We will use it by taking into account the sum of the two sides and thus considering only once the range $m_T < E \lesssim W/2$. We take the first group of data with $0 < p_T < 0.2$ from Fig. 11 and use an average $m_T^2 = 0.03$ BeV^2. Multiplying the cross sections by E and plotting the result vs $\mathscr{M}$ we get Fig. 12. Can these results be a manifestation of Eq. (17) only? No. The reason for the definite answer lies in the power of Eq. (17) that describes not only the p_L distribution for fixed W but also the W behaviour for any p_L. If that behaviour would be given for the 4-prongs case by Fig. 12 one should expect a strong increase in the 4-prongs cross section which is given by the integral of Eq. (17). We show the behaviour of the various cross sections in Fig. 13. Clearly no such growth is observed in the 4-prongs events. Hence we conclude that g must be a strongly varying function of its variables. Nevertheless we realize that the trend of the curves of Fig. 12 to become more peaked as the number of prongs increases can be correlated with the change in the behaviour of the relevant cross-sections in Fig. 13. This is a partial explanation of the second observation made at the beginning of this section. We conclude that the combination of two effects—

the probability amplitude g and the phase-space restrictions is intricately interwoven in the structure of the distributions ρ.

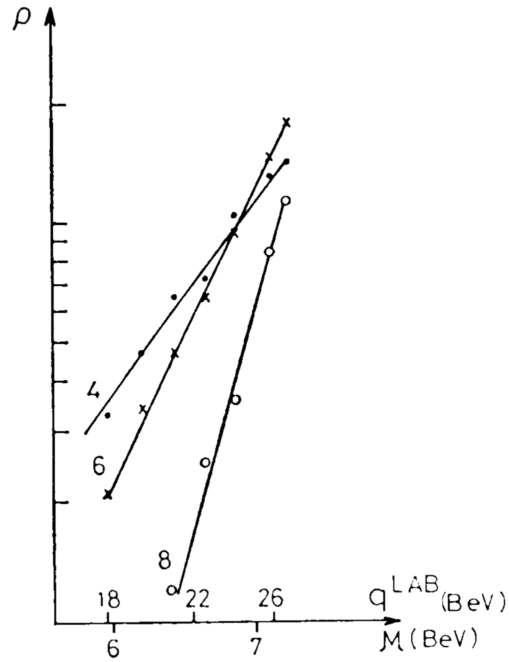

Fig. 12. Test of Eq. (17) showing the plot of $\rho_i(p_L)$ for the lowest p_T bin of Fig. 11 vs. $\mathcal{M}$. The equivalent q^{LAB} values are added for comparison with Fig. 13.

6. SCALING AND LIMITING FRAGMENTATION

Let us turn now to a discussion of the inclusive processes. First we have to have a sample of data to play with. We use the data of Smith, Sprafka and Anderson[19] who studied pp interactions at five different energies. Their results for the growth of the cross sections with energy were shown in Fig. 13. They also give the information about the distributions in p_T (integrated over p_L) and in p_L (integrated over p_T). They parametrize them as follows:

$$\frac{1}{\sigma}\frac{\partial\sigma}{\partial p_T} = \frac{4}{3\sqrt{\pi}} a_\perp^{5/2} p_T^{3/2} e^{-a_\perp p_T} \qquad \frac{1}{\sigma}\frac{\partial\sigma}{\partial p_L} = a_{||} e^{-a_{||} p_L} \tag{19}$$

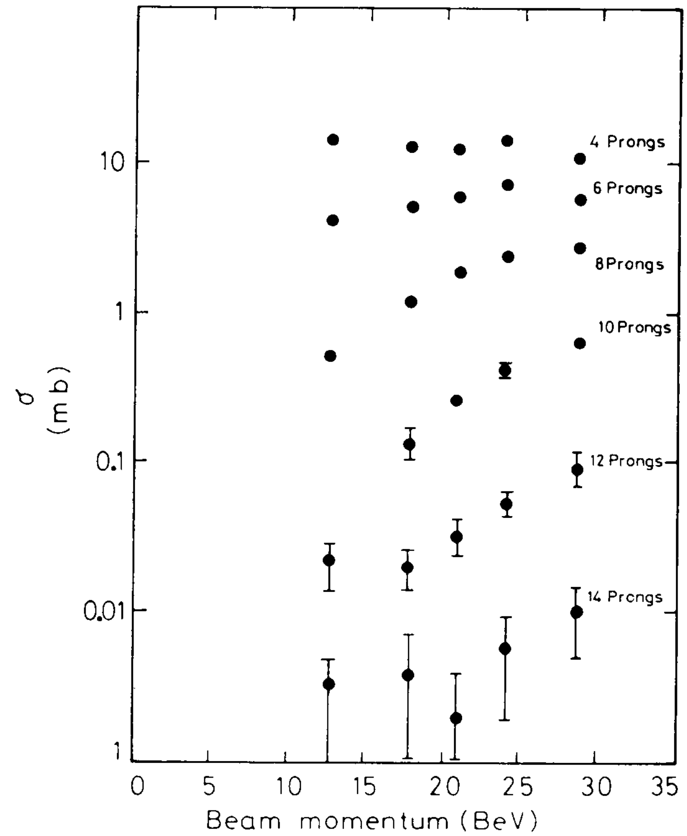

Fig. 13. Cross sections of pp collisions, from Ref. 19.

Their results for the various parameters are exhibited in Fig. 14. Ideally we would like to have the inclusive distribution for various p_T values. Until this becomes available we follow Chou and Yang[20] and look at the appropriately weighted sum of the 4, 6 and 8 prongs data using a constant $p_T = 0.2$ BeV. The resulting curves will be shown in the next figures and should be regarded as an approximation to the general features of the inclusive distributions in p_L averaged over p_T.

Once again we consider the π^- distribution in pp collisions. In Fig. 15 we show $\rho = E(d\sigma/dp_L)$ plotted vs the variable

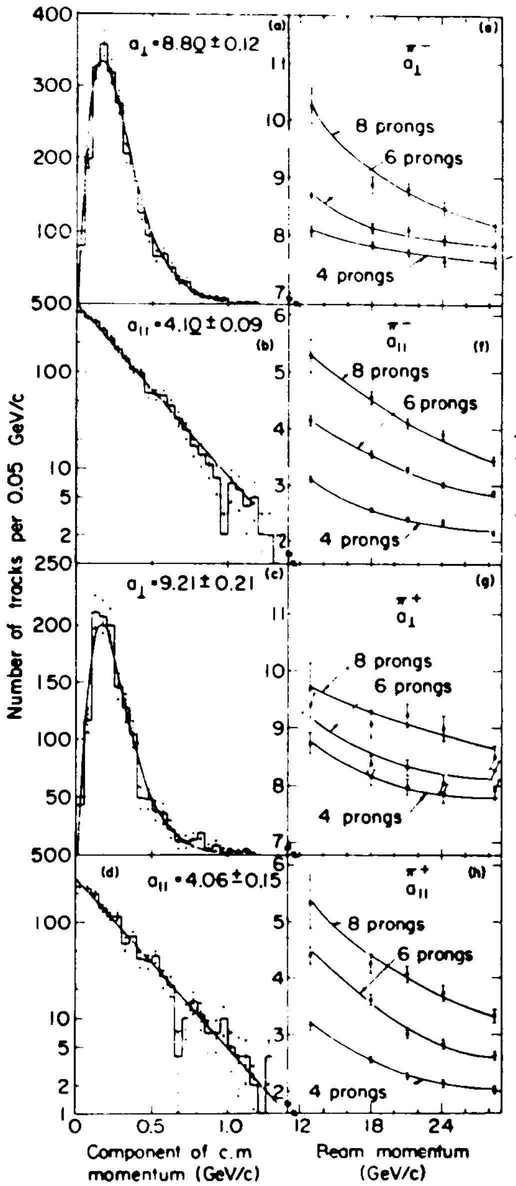

Fig. 14. Parameters of momentum distributions in *pp* collisions taken from Ref. 19.

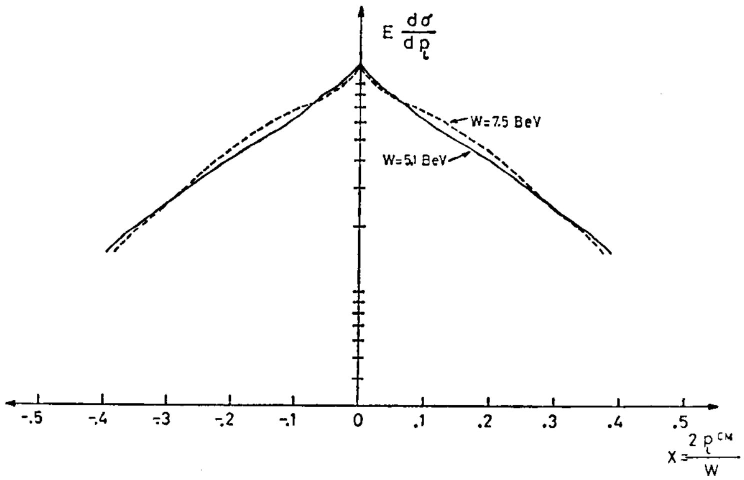

Fig. 15. The π^- distribution of pp reactions (constructed in the way which is described in the text) is shown for two different W values corresponding to lab energies of 12.9 and 28.4 BeV.

$x = 2p_L^{CM}/W$. We note the expected peak at the CM point ($p_L=0$) and the fact that for the two different incoming energies these two curves practically coincide. This verifies a suggestion by Feynman[21] that the inclusive distributions scale in x. This property of scaling leads to an interesting result for the average multiplicity that was noted and discussed by Bali et al.[22] As can be seen from Eq. (16)

$$\int \rho_i^T \frac{d^3p}{E} = \langle n_i \rangle \sigma_T \tag{20}$$

where $\langle n_i \rangle$ is the average multiplicity of particles of type i. If ρ_i^T scales in x then in p_L it has a range proportional to W. This leads to a logarithmic increase of the integral with W. Since σ_T is assumed to be constant the logarithmic increase of $\langle n_i \rangle$ follows. Bali et al.[22] have given a factorized expression for ρ_i (of the type $g(p_T)f(x)$) which can be regarded as a crude fit to the data and leads to consistent results for the values of $\langle n_i \rangle$.

An alternative way to look at the high energy processes was suggested by Benecke et al.[28] They suggested that these processes look simple when viewed in the target or the projectile frame of reference. We will discuss in the following just the target (LAB) frame but clearly things look similar in the projectile frame of reference. When viewed in this way one regards the outcoming particles as the results of the fragmentation of the two original particles into well-defined ratios of hadronic matter under the influence of the collision. The simplicity that we referred to lies in the proposition that the distribution of the outgoing particles reaches a limiting value that is independent of the original total energy of the collision (W). To test this proposal we use the same data that were used to obtain Fig. 15 and reproduce $d\sigma/dp_L^{LAB}$ in the target frame. This is shown in Fig. 16. Note that because we test the relation between two distributions in the same frame of reference it does not matter whether we use $d\sigma/dp_L^{LAB}$ or $\rho = E_L^{LAB}(d\sigma/dp_L^{LAB})$. We used the former in order to agree with Chou and Yang[20] who obtained this figure. We note that the two curves, drawn for two different incoming energies, agree over a wide range of momentum.

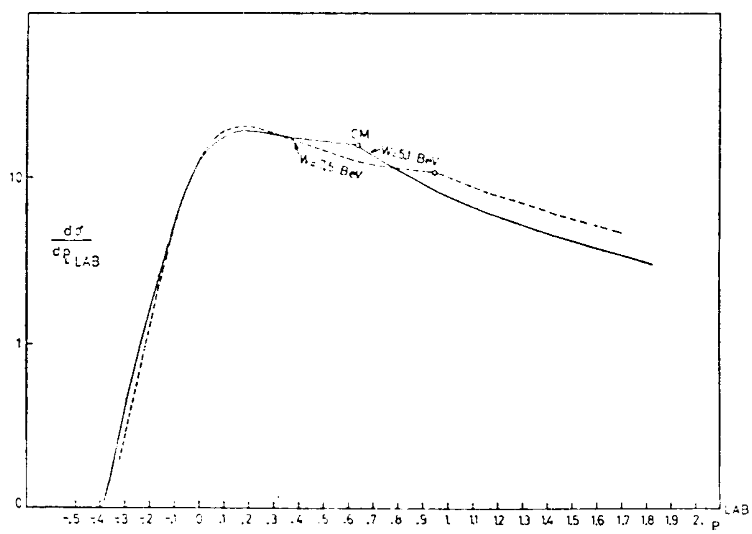

Fig. 16. $d\sigma/dp_L$ of the same distribution as in Fig. 15 plotted vs. p_L^{LAB} to show the limiting fragmentation behaviour. Because of the difference by a factor of E there is quite a distortion of the shape compared to Fig. 15. The CM peaks are sparious effects of the way we constructed the distributions using the exponential in Eq. (19).

Clearly if both Feynman's scaling and the limiting fragmentation ideas work they have to be consistent with one another. To show that this is indeed the case we note that under longitudinal boosts (see Eq. (11)) the ratios of expressions like $E - p_L$ (or $E + p_L$) for two different particles stay invariant. We look therefore at $E - p_L$ for the particle tested and for the target (whose energy in CM is $W/2$ and momentum in CM is $-q \approx -W/2$) and find

$$\xi = \frac{E^{\mathrm{CM}} - p_L^{\mathrm{CM}}}{\dfrac{W}{2} + q} = \frac{E^{\mathrm{LAB}} - p_L^{\mathrm{LAB}}}{M} \tag{21}$$

where M is the mass of the target. Note that for p_L^{CM} that are large in magnitude and negative ($p_L^{\mathrm{CM}} \ll -m_T$), namely those momenta that are in the direction of the target in the CM frame, one finds

$$\xi \approx \frac{E^{\mathrm{CM}} - p_L^{\mathrm{CM}}}{W} \approx \frac{-2p_L^{\mathrm{CM}}}{W} = -x \tag{22}$$

From (21) and (22) we learn that if ξ is the "true" scaling variable then the distributions will be independent of W when viewed in the LAB frame (Eq. (21)) and approximate scaling in x follows (Eq. (22)). Alternatively if x is the "true" scaling variable then the limiting fragmentation is an approximate (asymptotic) statement. In practice we are not yet in the situation of deep inelastic electron scattering where the search for the best scaling variable motivated many papers recently, but we may expect similar questions to motivate better measurements and further research in the hadronic high energy collisions.

The variable x can have both positive and negative values, whereas ξ can have positive values only. The particular problem that we discussed, $pp \to \pi^- \cdots$, is symmetric in x as shown in Fig. 15. Comparing Figs. 15 and 16 we see that the regions of low $|p_L^{\mathrm{CM}}|$ are better described by scaling in x. However in the region where $-x$ and ξ are comparable the difference between the two descriptions cannot be judged on the basis of our "data". The region where the x description is better corresponds to very low regions of ξ, namely to high p_L^{LAB} values. To emphasize this point we draw again the same data in Fig. 17, this time as a

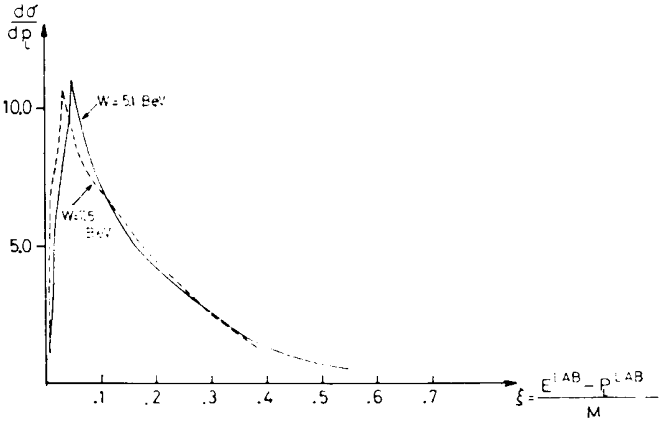

Fig. 17. Same distribution of Fig. 15 plotted vs ξ. See also caption of Fig. 16.

function of ξ. Chou and Yang[20] noted that since the values ξ_j of the various particles emitted in a process obey the relation

$$\sum_{all\ particles} \xi_j = 1 + \frac{E^{\mathrm{LAB}} - p_L^{\mathrm{LAB}}}{M}\Bigg|_{projectile} \approx 1 \quad (23)$$

that comes from energy-momentum conservation, the following sum rule follows

$$\sum_i \frac{1}{\sigma_T} \int \rho_i^T \xi \frac{d^3p}{E} = 1 \quad (24)$$

where the sum is over all types i of particles emitted. This sum rule emphasizes the region of high values of ξ where limiting fragmentation is applicable. It can be used to give some invariant meaning to the measure of the relative importance of the various hadronic fragments emitted in the collisions. The authors[20] called the contribution of each type of particle i to the sum rule (24) its "fragmentation fraction". They estimated the following fractions in pp collisions: The proton contributes 40%, the neutron 12%, all pions 40% and all kaons 5%. The relative importance of the proton is of course because it appears as a leading particle and therefore contributes characteristically to higher ξ values than the pions which are after all concentrated around the CM.

It should be noted that the inclusive distributions depend on three variables—W, p_L and p_T. In the present discussion we neglected the p_T dependence because of lack of data. We know already from Fig. 11 that there exists some correlation between the p_T and p_L distributions and it would be very interesting to know whether there exists a scaling variable that takes it into account. Clearly x is not the answer because it is independent of p_T, however ξ could be a good candidate (this regards only the shape of the distribution and not the overall magnitude that has a sharp p_T dependence). Hopefully we will soon have experimental data that will enable us to investigate these questions.

7. REGGEISTIC APPROACH TO INCLUSIVE DISTRIBUTIONS

An approach that discusses the inclusive data in the familiar Regge language was recently introduced by Mueller.[24] He pointed out that the inclusive distribution ρ^T can be regarded as a discontinuity in a six-point "forward scattering" amplitude (shown in Fig. 18) in an analogous fashion to the connection between the total cross section and the discontinuity of a forward scattering four-point function given by the optical theorem. For certain regions of the kinematical variables one can then assume dominance of Regge behaviour which leads to testable interesting predictions. We have first to introduce the kinematical variables. We know them already as p_L, p_T (neglecting the $\vec{p}_T$ direction because of cylindrical symmetry) and W. However it may be useful to recast them into new variables because of this new

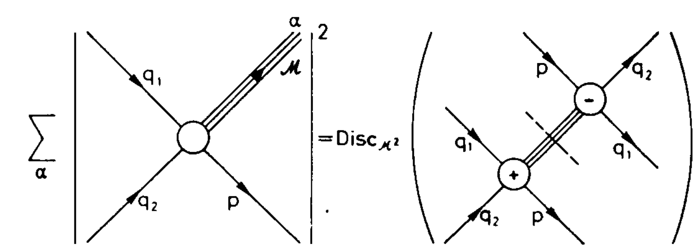

Fig. 18. Diagramatic representation of Mueller's generalized optical theorem[24] for inclusive distributions.

approach. One possible set of variables is given by the energies ν, ν_1 and ν_2 defined as follows

$$\nu = \frac{q_1 \cdot q_2}{M} \qquad \nu_1 = \frac{p \cdot q_1}{M} \qquad \nu_2 = \frac{p \cdot q_2}{M} \tag{25}$$

where we chose the same mass M for the target (q_1) and projectile (q_2). The generalization to other cases is straightforward. For further use we note the following connection between these variables and $E = p_0$ in the CM frame:

$$\frac{\nu_1 \nu_2}{m_T{}^2} = \frac{\nu}{2M} + \frac{E^2}{m_T{}^2} - \frac{1}{2} \tag{26}$$

Alternatively one may just use the known s, t, u variables

$$\begin{aligned} s &= (q_1 + q_2)^2 = 2M^2 + 2M\nu = W^2 \\ t &= (q_1 - p)^2 = M^2 + \mu^2 - 2M\nu_1 \\ u &= (q_2 - p)^2 = M^2 + \mu^2 - 2M\nu_2 \end{aligned} \tag{27}$$

Note however that all three are independent since their sum includes a variable which we met before

$$\begin{aligned} s + t + u &= 2M^2 + \mu^2 + \mathcal{M}^2 \\ \mathcal{M}^2 &= W^2 - 2EW + \mu^2 \end{aligned} \tag{28}$$

The two kinematical regions discussed by Mueller[24] embed the dynamics contained in parts a and b of Fig. 19. Figure 19a applies to small ν_1 values, namely the "fragmentation" region of the target q_1. This corresponds also to low t and large s and u values. The discontinuity of this amplitude is supposed to be dominated by Pomeron exchange and one finds[24]

$$\rho^T = E\frac{d^3\sigma}{d^3p} \propto \frac{1}{\nu}\nu_2^{\alpha(0)} f(\vec{p}^{\,\mathrm{LAB}}) \xrightarrow[\alpha = 1]{} f(\vec{p}^{\,\mathrm{LAB}}) \tag{29}$$

which is the statement of limiting fragmentation. One may of course expect corrections due to lower lying trajectories. The leading corrections will behave like $\nu^{-\frac{1}{2}} \approx W^{-1}$. Chan et al.[25] pointed out that one should expect this effect only in non-exotic channels. Ellis et al.[26] emphasized that the limiting fragmentation

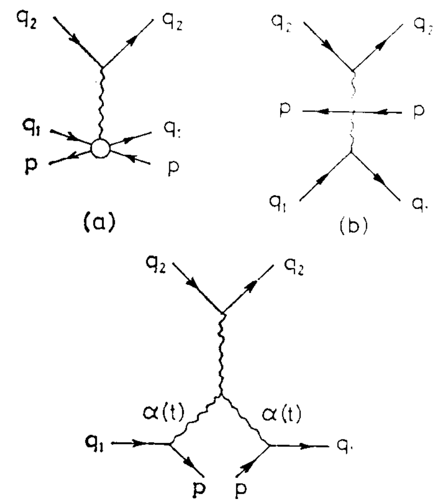

Fig. 19. Three particular Pomeron exchange diagrams contributing to the inclusive distributions.

limit is quickly obtained only if both $q_1 + q_2$ and $q_1 + q_2 + \bar{p}$ correspond to exotic combinations (thus $pp \to \pi^- + \cdots$ and $K^+p \to \pi^- + \cdots$ are regarded exotic whereas $\pi^+p \to K^- + \cdots$ is non-exotic). It will take still some time until one has accurate enough data to investigate such effects.[27]

Figure 19b applies to an extreme pionization limit. One requires large ν, ν_1 and ν_2 which is equivalent to large s, t and u. A double Regge exchange description leads then to a discontinuity of the 6-point amplitude given by

$$A = \nu_1^{\alpha_1} \nu_2^{\alpha_2} f(m_T) \tag{30}$$

which, in the limit of two Pomeron exchange, results in

$$\rho^T \propto \frac{1}{\nu} A = \frac{(\nu_1 \nu_2)^{\alpha(0)}}{\nu} f(m_T) \xrightarrow[\alpha=1]{} \frac{m_T^2}{2M} f(m_T) \tag{31}$$

In the last step we used Eq. (26) neglecting $E \approx m_T$ in the pionization limit. The result (31) implies complete independence on the longitudinal momentum in accordance with the expectations of all theories quoted at the end of Section 5. At what energies (ν) can we expect this effect to show up? Equation (26) tells us that at $E = m_T$ one finds that $\nu_1 = \nu_2 = m_T[(\nu + M)/2M]^{1/2}$. This means that for reasonable ν values (around 30 BeV) one finds ν_1 and ν_2 of the order of 1 BeV.

Can we expect for such small ν_1 and ν_2 values a Pomeron behaviour? Figure 19b resembles a product of two πp scattering amplitudes. They are known not to be yet at their Pomeron limit at energies of 1 BeV. It may be that this explains why we do not yet see a flat distribution in z at this point. Judging from πp scattering a factor of 4 in available ν might do it. It should be emphasized that the intuitive arguments that we used here are subject to criticism since the behaviour of the two Pomeron coupling is still an enigma. Moreover it is known from the usual multi-Regge formalism that a similar coupling tested there is presumably very weak.[6] The ISR and NAL data may tell us soon whether diagrams b are present by comparing data from higher and lower energies near $x \approx 0$.

Finally let us concentrate on Fig. 19c. It was recently suggested by De Tar et al.[28] and can apply to regions where both s and $s/\mathcal{M}^2$ are very big. We note that

$$\frac{\mathcal{M}^2}{s} = \frac{W^2 - 2WE + m^2}{W^2} \approx 1 - x \tag{32}$$

hence this is applicable in the region where $x \approx 1$ and s is very big. This diagram is a special case of diagram a. It includes usual Pomeron exchange at $\alpha = 1$, which stands for the diffractive sum over all the particles, and a particular Regge type coupling valid for small t values. In the region where this diagram is applicable it leads to

$$-\frac{d^2\sigma}{dt\,dx} = \left(\frac{s}{\mathcal{M}^2}\right)^{2\alpha(t)} \beta(t) \frac{(\mathcal{M}^2)^{\alpha_P(0)}}{s} \tag{33}$$

A look at Fig. 15 convinces us that the π data vanish quickly as x grows. We may however hope that if we look instead at $pp \to p + \cdots$ then an appreciable signal near $x \approx 1$ is obtained since the outgoing proton is a leading particle. This is indeed the case. In the language of Eq. (33) we find that an outgoing pion corresponds to baryon exchange and an outgoing proton to a meson trajectory in agreement with the dominance of the latter. Figure 20 is a recent compilation of $pp \to p + \cdots$ data by Edelstein, Rittenberg and Rubinstein.[29] The quantity plotted here differs from Eq. (33) by a factor of $\mathcal{M}$. Its scaling in $\mathcal{M}^2/s \approx 1-x$ is evidence of the importance of P' exchange with $\alpha(0) \approx \frac{1}{2}$ relative to the Pomeron exchange of Eq. (33). This effect is connected to the rather low $\mathcal{M}^2$ values obtainable at present for $x \to 1$ and enables us to see dual effects in inclusive distributions.

The studies of particular limits of the six-point function that describes the inclusive amplitude do not lead in a natural way to the scaling property in x that seems to hold over large regions

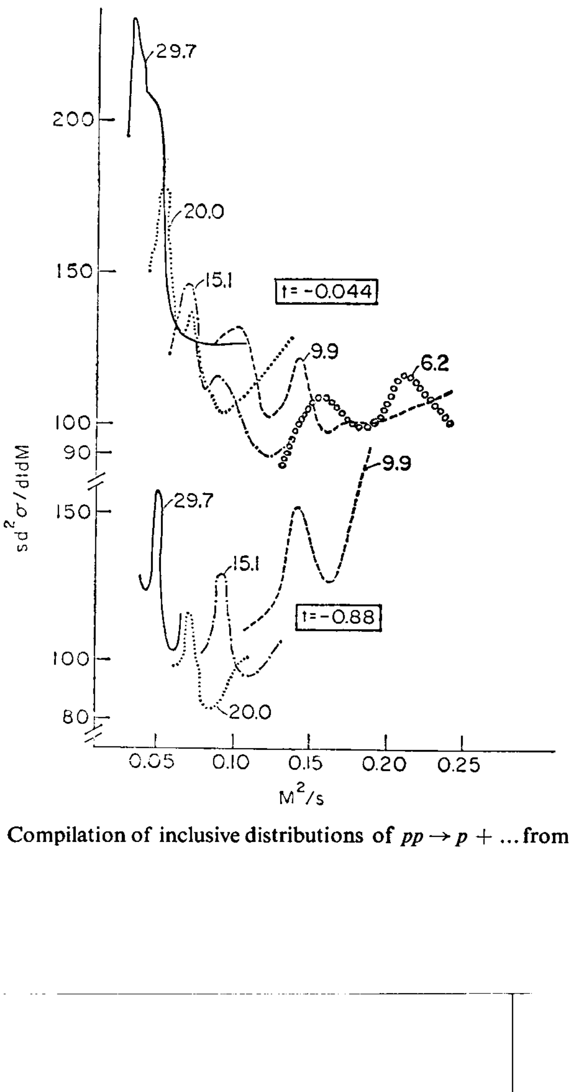

Fig. 20. Compilation of inclusive distributions of $pp \to p + \ldots$ from Ref. 29.

at presently available energies, as we saw in the previous section. Therefore it does not explain the functional forms of Figs. 15, 16 and 17. We may however hope that the recent general interest in the subject will lead to a better understanding of the many details of the various distributions. The six-point function can be studied in the Veneziano model.[30, 31] Although it does not contain Pomeron exchanges it leads to some interesting results, the most striking being an asymptotic scaling in x and $e^{-4}p_T^2$ behaviour of the transverse momentum distribution for low p_L values. This Gaussian distribution is not in perfect agreement with the experimental data of Fig. 14. If approximated by a Gaussian at low p_L values one finds $e^{-10}p_T^2$ and even stronger slopes. Nevertheless it is interesting to see that the harmonic behaviour of the Veneziano amplitudes leads to a natural cutoff in the transverse momentum of the emitted particles.[31]

8. CORRELATIONS

Clearly the next topic to discuss after the single particle distributions is the two particle correlation. Because of the embryonic stage of our knowledge of this important question we devote to it only this one and last section.

If one looks at reactions with low multiplicity then one can distinguish particular exchanges[32] as well as particular resonances that are produced. However the average multiplicity of particles produced at conventional accelerator energies is of the order of 6. In order to observe fair correlations in such reactions, one has first to restrict the set of particles that is analyzed. Otherwise a correlation between a pair of particles may be washed out by the vast number of possible combinations. Thus one may ask about correlations between a pion and a leading particle, or between two neighbouring pions on the rapidity scale. Such correlations are presumably constant or slowly varying with the total energy W. Alternatively one may ask how does a correlation between two pions change as the distance between them in rapidity changes. This correlation function can be defined as

$$\tau_{ij}(\vec{p}_{Ti}z_i\vec{p}_{Tj}z_j) = \frac{\rho_{ij}(\vec{p}_{Ti}z_i\vec{p}_{Tj}z_j)}{\sigma_T} - \frac{\rho_i(p_{Ti}z_i)}{\sigma_T}\frac{\rho_j(p_{Tj}z_j)}{\sigma_T} \tag{34}$$

where ρ_{ij} is defined in an analogous fashion to ρ_i. Wilson[16] suggested that this correlation dies out exponentially as the difference in rapidity $(z_i - z_j)$ increases. These questions can be formulated for inclusive reactions and we may expect to see in the near future experimental and theoretical progress along these lines.

An independently interesting question is whether the overall correlation

$$\tau_{ij} = \int \tau_{ij}(p_i p_j) \frac{d^3 p_i}{E_i} \frac{d^3 p_j}{E_j} \tag{35}$$

is big or small. Can the Poisson-type distributions mentioned in Section 2 indicate that the size of the overall correlation is small? A test of the type of distribution to be used is given in Fig. 21 which consists of a compilation by Wang[33] and several theoretical curves. The curve W^1 is a Poisson distribution in $\pi^+\pi^-$ pairs and presents therefore the case of strong correlation. The solid curve corresponds to a Bessel distribution.[34] This results from the product of two independent emissions (Poisson in π^+ and π^- separately), subject to the condition of total zero charge, and could lead to negligible correlations between π^+ and π^-. Although it looks compelling to assume that the overall correlation is small it is difficult to give exact estimates of it on the basis of available data which are consistent with different interpretations.

Can pions be emitted independently? There are three different types of constraints that work against it:

1) Overall momentum conservation (phase space).

2) Conserved quantum numbers (charge, parity, charge configuration).

3) Isospin conservation.

The first constraint cannot be avoided; however it is not crucial since the pions' distribution is anyway concentrated around the

CM and dies out quickly toward the edges of phase space. The points 2 and 3 can be simply avoided in a model that produces pion pairs with vacuum quantum numbers ($I = 0\ J^{PC} = 0^{++}$). Although this looks like the simplest way out it is not necessarily Natures' solution to the problem. An alternative like independent

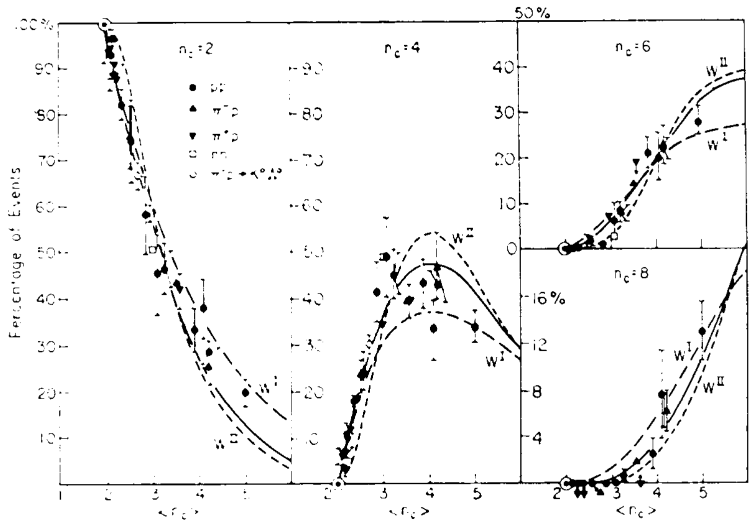

Fig. 21. Theoretical distributions of cross sections for charged particle emission are compared with Wang's compilation of inelastic productions data[33]. W^I and W^{II} are different types of Poisson distributions from Ref. 33 and the solid curve is a Bessel distribution from Ref. 34.

and coherent emission of pions, which is the closest to a classical radiation of a pion field, may still serve as a crude approximation.[35] If the pions can be thought of in any approximation as independently produced one should expect the π^0 spectrum to be independent of the charged pions. A recent experiment[36] looked at such a question and the results are given in Fig. 22. They are of course still inconclusive and can be consistent with either a constant or a strong varying function based on strong correlations.[37]

The questions that we raised are only a small sample of all possible puzzles in the high multiplicity reactions. We may expect that the coming years will see more efforts, in both experiment and theory, directed towards solving these problems and understanding the physics of many particle production.

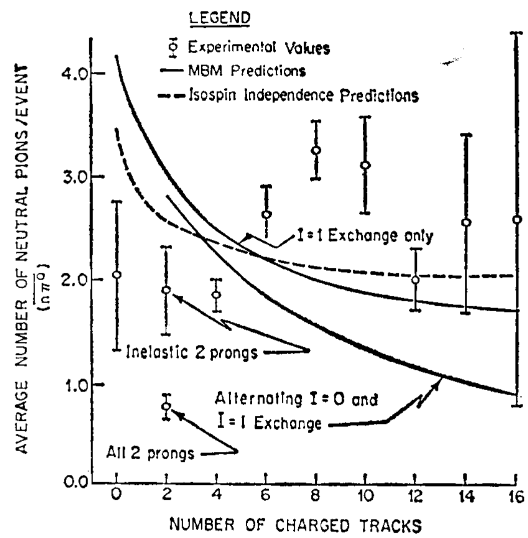

Fig. 22. The average number of π^0 produced in π^-p reactions at 25 BeV vs the number of charged particles. Taken from Ref. 36.

9. ACKNOWLEDGEMENTS

Thanks are due to many of my colleagues at Tel Aviv University, and in particular to S. Nussinov, for many helpful discussions

REFERENCES

1. J. W. Waters, W. D. Walker, A. R. Erwin, J. W. Elbert, University of Wisconsin paper submitted to Lund Conference, 1969.
2. R. Honecker et al., ABBCCHW Collaboration, *Nucl. Phys.* **B13**, 571 (1969); M. Deutschmann et al., ABBCCHW Collaboration, submitted to Kiev Conference, 1970.
3. L. W. Jones et al., *Phys. Rev. Lett.* **25**, 1679 (1970).
4. L. Bertochi, S. Fubini and M. Tonin, *Nuovo Cim.* **25**, 626 (1962); D. Amati, S. Fubini and A. Stanghellini, *Nuovo Cim.* **26**, 896 (1962).
5. T. W. B. Kibble, *Phys. Rev.* **131**, 2282 (1963). K. A. Ter Martirosyan, *Zh. Eksperim. i. Teor. Fiz.* **44**, 341 (1963). [translation: *Soviet Phys.—*

JETP **17**, 233 (1963)]. F. ZACHARIASEN AND G. ZWEIG, *Phys. Rev.* **160,** 1322, 1326 (1967). G. F. CHEW AND A. PIGNOTTI, *Phys. Rev.* **176,** 2112 (1968).
6. See e.g. R. LIPES, G. ZWEIG AND W. ROBERTSON, *Phys. Rev. Lett.* **22,** 433 (1969).
7. CHAN HONG-MO, J. LOSKIEWICZ AND W. W. M. ALLISON, *Nuovo Cim.* **57A,** 93 (1968).
8. C. LOVELACE, review talk at Regge Pole Conference, U.C. Irvine Calif. (1969).
9. G. F. CHEW, T. ROGERS AND D. R. SNIDER, *Phys. Rev.* **D2,** 765 (1970).
10. S. FUBINI, in *Strong Interactions and High Energy Physics,* (Scottish Universities' Summer School, 1963), edited by R. G. Moorhouse, Oliver & Boyd, 1964, p. 259.
11. H. W. WYLD, JR., University of Illinois, Urbana preprint ILL-(TH)-71-2.
12. D. M. TOW, *Phys. Rev.* **D2**, 154 (1970).
13. H. D. I. ABARBANEL, G. F. CHEW, M. L. GOLDBERGER AND L. M. SAUNDERS, *Phys. Rev. Lett.* **25,** 1735 (1970).
14. J. D. HANSEN, W. KITTEL AND D. R. O. MORRISON, *Nucl. Phys.* **B25,** 605 (1971). T. HOFMOKL AND A. WROBLEWSKI, *Phys. Lett.* **31B,** 391 (1970).
15. J. GRUNHAUS, D. HORN AND S. NUSSINOV, unpublished results.
16. K. G. WILSON, Cornell preprint, CLNS-131.
17. H. CHENG AND T. T. WU, *Phys. Rev. Lett.* **23,** 1311 (1969).
18. R. R. KINSEY, T. W. MORRIS, R. S. PANVINI, paper submitted to the Kiev Conference, 1970.
19. D. B. SMITH, R. J. SPRAFKA AND J. A. ANDERSON, *Phys. Rev. Lett.* **23,** 1064 (1969).
20. T. T. CHOU AND C. N. YANG, *Phys. Rev. Lett.* **25,** 1072 (1970). Note that our ρ^T differs from their $\bar{\rho}_1$ by a factor of E.
21. R. P. FEYNMAN, *Phys. Rev. Lett.* **23,** 1415 (1969) and in *High Energy Collisions,* by C. N. YANG ET AL. ed., Gordon and Breach, New York, 1969, p. 237.
22. N. F. BALI, L. S. BROWN, R. D. PECCEI AND A. PIGNOTTI, *Phys. Rev. Lett.* **25,** 557 (1970).
23. J. BENECKE, T. T. CHOU, C. N. YANG AND E. YEN, *Phys. Rev.* **188,** 2159. (1969).
24. A. H. MUELLER, *Phys. Rev.* **D2,** 2963 (1970). We do not use his $O(2, 1)$ expansion methods. For later developments in this formalism see, e.g H. D. I. ABARBANEL, Princeton preprints.
25. CHAN HONG-MO, C. S. HSUE, C. QUIGG AND J. M. WANG, *Phys. Rev. Lett.* **26,** 672 (1971).
26. J. ELLIS, J. FINKELSTEIN, P. H. FRAMPTON AND M. JACOB, *Phys. Lett.* **35B,** 227 (1971).
27. For recently compiled data we refer the reader to Ref. 22 for $pp \to \pi^+ \ldots$ and to the following two papers for $\pi^- p \to \pi^\pm + \cdots$: R. W. ANTHONY,

C. T. COFFIN, E. S. MEANLEY, J. E. RICE, K. M. TERWILLINGER AND N. R. STANTON, *Phys. Rev. Lett.* **26**, 38 (1971); M. S. CHEN, L. L. WANG AND T. F. WONG, *Phys. Rev. Lett.* **26**, 280 (1971).
28. C. E. DETAR, C. E. JONES, F. E. LOW, J. H. WEIS, J. E. YOUNG AND C. I. TAN, *Phys. Rev. Lett.* **26**, 675 (1971).
29. R. EDELSTEIN, V. RITTENBERG AND H. R. RUBINSTEIN, preprint.
30. C. E. DETAR, K. KANG, CHUNG I. TAN AND J. H. WEIS, paper submitted to the conference. G. VENEZIANO preprint, M. VIRASORO preprint.
31. S. H. NOSKOWICZ AND L. SUSSKIND, preprint TAUP-186-70.
32. See e.g. the review paper by L. VAN HOVE, *Physics Reports* **1**, 347 (1971).
33. C. P. WANG, *Phys. Rev.* **180**, 1463 (1968).
34. D. HORN AND R. SILVER, *Phys. Rev.* **D2**, 2082 (1970).
35. D. HORN AND R. SILVER, CERN preprint TH 1226, to be published in *Annals of Physics*, **66** (1971).
36. J. W. ELBERT ET AL., *Nucl. Phys.* **B19**, 85 (1970).
37. L. CANESCHI AND A. SCHWIMMER, *Phys. Lett.*, **33B**, 577 (1970).

DISCUSSION

M. VIRASARO

I would like you to comment whether the distribution for inclusive reactions $f(x, p_T)$ factorizes in $f(x)g(p_T)$ experimentally.

D. HORN

It can be used as an approximation. However there exists a correlation between the distribution in p_L (or x) and the distribution in transverse momentum. At $p_L = 0$ (the CM point) one finds a minimum in p_T. I would say that if you want to have something that is true within 20% then you can use that factorization. If you want it to be better than that then you have to put in a correlation between the two.

S. FUBINI

Let me use the privilege of being Chairman to also answer your question. It was a multi-peripheral model which actually first gave a result that factorized. If you improve on that, there may be a lack of factorization, but it is the original multi-peripheral model which gave the logarithmically rising multiplicity, the factorization and the scaling in dp/E and it was clear that all are related because they come from the same model essentially.

D. HORN

Did you ask about theory or about experiment?

M. VIRASARO

I am asking about inclusive experiment.

D. HORN

In Fig. 11 we saw the correlations between p_T and p_L distributions that show the property that I mentioned above. These correlations are shown for 4, 6 and 7 prongs and hold therefore also for the inclusive distributions.

L. SUSSKIND

With respect to Virasaro's question is it not true that the average transverse momentum of a pion in an inclusive case is independent of p_T for a wide range of p_L?

D. HORN

At least not near the CM region.

D. MORRISON

I think that the answer that Horn gave to the previous two questions applies experimentally also to inclusive reactions. That is to say broadly speaking you can factorize the distribution, but as soon as you start looking in detail there are effects due to resonances, to phase space and things like that which spoil this factorization. These are second order effects which make the p_T distribution vary with p_L.

H. HARARI

You started by listing five prominent features of multiparticle processes. I would like to add another crucial experimental fact which should perhaps be considered in future theories. I refer to the very low average subenergy for a neighbouring pair of particles along a longitudinal momentum plot. The average subenergy for a pair of pions is 550–600 MeV and it does not increase with energy, if the multplicity increases logarithmically. This fact is as striking as the cutoff in transverse momentum, and is probably related to it. The low subenergy is, however, orthogonal to the spirit of the multiperipheral model (although duality may serve this last model in this case).

M. BANDER

In discussing the approach to limiting distributions from the angular momentum point of view the question arises what is s_0 in $(s/s_0)^\alpha$, could $s_0 \sim p_L^2$? Then all Regge poles would contribute to this limit. This may occur in inelastic electron scattering where $s_0 \sim Q^2$.

D. HORN

My feeling is that when we look at something like a double Pomeron exchange description of pionization we should measure the ν in BeV thus comparing half the diagram to the familiar situation of pion nucleon scattering.

H. LIPKIN

Is there any reason for suppression of kaon production?

D. HORN

An $SU(3)$ violating term like $m\pi/(m_K)^2$ can always do it. I think that it is not well understood because we do not have a good description of the whole mechanism. The thermodynamic school of thought expects of course a sharp decrease of production cross sections for increasing masses